EPR Spectroscopy, Theory

Christopher C Rowlands and Damien M Murphy, Cardiff University, UK

This article is reproduced from the previous edition, volume 1, pp 445–456, © 1999, Elsevier Ltd.

Symbols

a	hyperfine coupling constant
A_0	theoretical isotropic hyperfine coupling constant
A	hyperfine tensor
g	g factor
g_e	g factor of the free electron
g_J	Landé g factor
g_N	nuclear g factor
$g_\parallel$ and $g_\perp$	refer to the parallel and perpendicular values with respect to axis of symmetry
g_{xx}, g_{yy}, g_{zz}	refer to values in the respective crystallographic directions
h	Planck's constant
$\hbar$	$h/2\pi$
I	nuclear spin quantum number
J	total angular momentum
k	Boltzman constant
L	orbital angular momentum vector
m_e	mass of the electron
N_L and N_U	electron populations in the lower and upper energy levels respectively
r	distance between the spins
r	vector relating electron and nuclear moments
S	electron spin quantum number
S_z	vector of the electron spin quantum number in the z direction
T_{1e} and T_{2e}	spin–lattice and spin–spin relaxation times, respectively
α and β	refer to electron spin
μ	magnetic moment
μ_B	Bohr magneton
μ_N	nuclear magneton
ν	frequency

This article will discuss the concept and outline the theory of electron paramagnetic resonance (EPR), sometimes known as electron spin resonance (ESR), spectroscopy. Paramagnetism arises as a consequence of unpaired electrons present within an atom or molecule. It can be said that EPR is the most direct and sensitive technique to investigate paramagnetic materials. It will not be possible within this article to fully expound on all the theoretical aspects of EPR and so the reader is encouraged to refer to the excellent texts listed in the Further Reading section.

Consequently this work is aimed at professional scientists who would like to expand their knowledge of spectroscopic techniques and also at undergraduates with the intention of allowing them to fully appreciate the scope, versatility and power of the technique.

Basic Principles of the EPR Experiment

The electron is a negatively charged particle that moves in an orbital around the nucleus and so consequently has orbital angular momentum. It also spins about its own axis and therefore has a spin angular momentum given by

$$\text{spin angular momentum} = h/2\pi[S(S+1)]^{1/2} \qquad [1]$$

where S is called the spin quantum number, with a value of $\frac{1}{2}$, and h = Planck's constant (6.626×10^{-34} Js). If we restrict ourselves to one specified direction, the z direction, then the component of the spin angular momentum can only assume two values and consequently $S_z = M_S h/2\pi$. The term M_S can have $(2S+1)$ different values of $+S$, $(S-1)$, $(S-2)\ldots(-S)$. If the possible values of M_S differ by one and range from $-S$ to $+S$ then the only two possible values for M_S are $\frac{1}{2}$ and $-\frac{1}{2}$.

Associated with the electron spin angular momentum is a magnetic moment μ and it is related to the spin as follows

$$\mu = g_e h/4\pi m_e[S(S+1)]^{1/2} \qquad [2]$$

where m_e = mass of electron, e = electron charge, S = spin quantum number and g_e is the spectroscopic factor known as the g factor (which has a value of 2.0023 for a free electron). The above equation can be rewritten as

$$\mu = -g_e \mu_B \, S/\hbar \qquad [3]$$

where $\mu_B = eh/2m_e$ and $\hbar = h/2\pi$. The z axis component μ_z will then be

$$\mu_z = -g_e \mu_B M_S \qquad [4]$$

μ_B is the Bohr magneton and has the value $9.2740 \times 10^{-24}\,\mathrm{J\,T^{-1}}$. The negative sign arises because of the

negative charge on the electron which results in the magnetic dipole being in the opposite direction to the angular momentum vector. The electron is restricted to certain fixed angular positions that correspond to the z component of the spin angular moment; S_z is a half integral number (M_S) of $\hbar/2\pi$, units. Since $S = \frac{1}{2}$ then $[S(S+1)]^{1/2}$ cannot be $\frac{1}{2}$ and consequently the spin angular momentum vector $\boldsymbol{s}$ and the magnetic moment vector $\boldsymbol{\mu}$ can never be aligned exactly in the field direction and they maintain a constant angle θ with the z axis and hence the applied field (**Figure 1**).

Hence, for a single unpaired electron, where $S = \frac{1}{2}$, the magnitude of the spin angular momentum along the z axis will be given by $+\hbar/2$ and $-\hbar/2$. For a free electron the spin angular momentum can have two possible orientations and these give rise to two magnetic moments or spin states of opposite polarity. In the absence of an external magnetic field the two spin states are degenerate. However, if an external magnetic field is applied then the degeneracy is lifted, resulting in two states of different energy. The energy of the interaction between the electron magnetic moment and the external magnetic field is given by

$$E = -\mu_z B \qquad [5]$$

where B = the strength of external magnetic field and μ_z = magnetic dipole along the z axis. In quantum mechanics the μ vector is replaced by the corresponding operator leading to the following Hamiltonian

$$H = -g_e \mu_B \boldsymbol{B} \boldsymbol{S}_z \qquad [6]$$

so that the energy is given by $E = -g_e\, \mu B M_S B$. For a single unpaired electron $M_S = \pm\frac{1}{2}$ and this gives rise to two energy levels known as Zeeman levels. The difference between these two energy levels is known as the Zeeman splitting (see **Figure 2**):

$$E_1 = \tfrac{1}{2} g_e \mu_B B \quad M_S = +\tfrac{1}{2} \quad \alpha \text{ spin} \uparrow \qquad [7]$$

$$E_2 = \tfrac{1}{2} g_e \mu_B B \quad M_S = -\tfrac{1}{2} \quad \beta \text{ spin} \downarrow \qquad [8]$$

Since $\Delta E \propto B$, the difference between the two energy levels is directly proportional to the external applied magnetic field. Transitions between the two Zeeman levels can be induced by the absorption of a photon of energy, $h\nu$, equal to the energy difference between the two levels:

$$\Delta E = g_e \mu_B B = h\nu \qquad [9]$$

where h = Planck's constant and ν = frequency of electromagnetic radiation. The existence of two Zeeman levels, and the possibility of inducing transitions from the lower energy level to the higher energy level, is the very basis of EPR spectroscopy. We can see, therefore, that the position of absorption varies directly with the applied magnetic field. EPR spectrometers may operate at different fields and frequencies (two common frequencies being $\sim$9.5 and $\sim$35 GHz, known as X and Q band respectively). It is therefore far more convenient to refer to the absorption in terms of its g value:

$$g = \Delta E/\mu_B B = h\nu/\mu_B B \qquad [10]$$

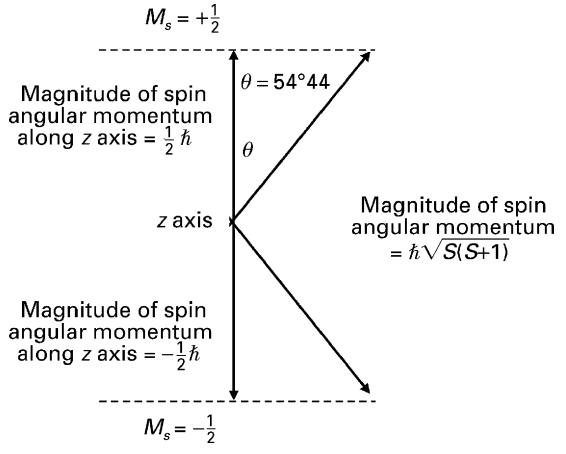

Figure 1 Allowed values of the magnitude of the spin angular momentum along the z axis for $S = \frac{1}{2}$.

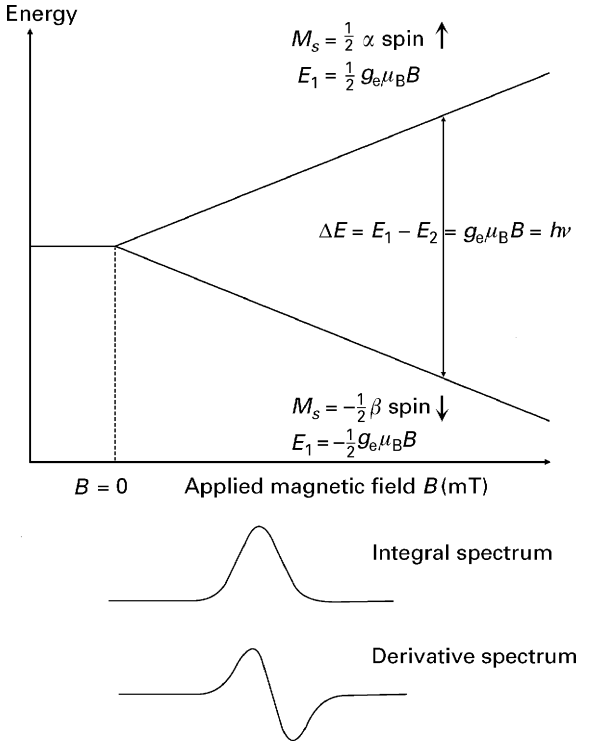

Figure 2 The Zeeman energy levels of an electron ($S = \frac{1}{2}$) in an applied magnetic field for a fixed microwave frequency.

Larmor Precession, Spin Populations and Relaxation Effects

It was noted above that the two spin states were at a constant angle to the z axis. However, in the presence of a magnetic field, the magnetic moment of the electron cannot align with the applied field and a turning couple is set up which results in a precession of the spin states around the z axis (**Figure 3**). This gives a physical mechanism by which spins can interact with electromagnetic radiation. When the magnetic component of the microwave radiation, which is orthogonal to the applied field, is at a frequency equal to that of the *Larmor precession* then the two are said to be in resonance, and energy can be transferred to the electron, inducing $\Delta M_S = \pm\frac{1}{2}$ transitions.

The incident radiation induces transitions not only from the lower to the higher energy states but can also induce emission with equal probability. Consequently the extent of absorption will be proportional to the population difference between the two states. At thermal equilibrium the relative *spin populations* of the two Zeeman levels is given by a Boltzmann equation:

$$N_U/N_L = e^{-\Delta E/kT} \quad [11]$$

where k = Boltzmann constant, T = absolute temperature (K), N_L = number of electrons in the lower level, N_U = number of electrons in the higher level and ΔE = difference in energy between the two energy levels. At room temperature (300 K) and in a magnetic field of 300 mT the populations of the two Zeeman levels are almost equal, but a slight excess exists in the lower level and it is this that gives rise to a net absorption. However, this would very quickly lead to the disappearance of the EPR signal as the absorption of energy would equalize these two states. For the experiment to proceed there has to be a process by which energy is lost from the system. Such processes are known as *relaxation processes*.

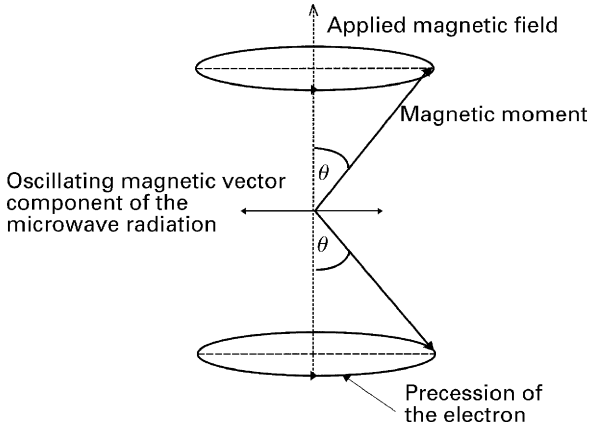

Figure 3 Two allowed electron spin orientations and the corresponding Larmor precession for $S = \frac{1}{2}$.

To maintain a population excess, electrons in the upper level must be able to return to their low energy state. Therefore they must be able to transfer their excess spin energy either to other species or to the surrounding lattice as thermal energy. The time taken for the spin system to lose $1/e$ of its excess energy is called the relaxation time. Two such relaxation processes are:

a. spin–lattice relaxation (T_{1e}): this process is due to lattice motions such as molecular tumblings in solids, liquids and gases which have a frequency comparable to that of the Larmor precession and this provides a pathway which allows the electron's excess energy to be transferred to the surroundings.
b. spin–spin relaxation (T_{2e}): the excess spin energy is transferred between paramagnetic centres through either dipolar or exchange coupling, from one molecule to another. This mode of relaxation is important when the concentration of paramagnetic species is high (spins are close together). If the relaxation time is too fast then the electrons will only remain in the upper state for a very short period of time and give rise to a broadening of the spectral line width as a consequence of Heinsenberg's uncertainty principle.

In general $T_{1e} > T_{2e}$ and the line width depends only on the spin–spin interactions (T_{2e}). However, if, in certain circumstances, both spin–spin and spin–lattice relaxations contribute to the EPR line width (ΔH), then the resonance line width can be simply written as

$$\Delta H \propto 1/T_{1e} + 1/T_{2e} \quad [12]$$

When T_{1e} becomes very short, below $\sim 10^{-7}$ s, its effects on the lifetime of the species in a given energy level makes an important contribution to the line width. In some cases the EPR lines are broadened beyond detection. The term T_{1e} may also be inversely proportional to the absolute temperature ($T_{1e} \propto T^{-n}$) with n depending on the precise relaxation mechanism. In such cases, cooling the sample increases T_{1e} and usually leads to detectable lines. For this reason, EPR experiments are frequently recorded at liquid nitrogen (77 K) or helium (4 K) temperatures.

Basic Interaction of the Electron with Its Environment

An expression for the spin state energies of an electron whose only interaction was with an applied magnetic field (a free electron) was derived above (eqn [6]). This represents an idealized model as in the real situation the electron suffers a variety of electrostatic and magnetic interactions which complicate the resonances. Consequently we must be able to account for these deviations. Magnetic resonance spectroscopists seek to characterize

and interpret EPR spectra and these deviations quantitatively using a device known as a *spin Hamiltonian*. The EPR spectrum is essentially interpreted as the allowed transitions between the eigenvalues of this spin Hamiltonian. The Hamiltonian contains terms which reflect the interactions of the spins of electrons and nuclei with the applied magnetic field and with each other, e.g.

$$\boldsymbol{H} = \mu_B \boldsymbol{B}\boldsymbol{g}\,\boldsymbol{S} + \Sigma_j \boldsymbol{I}\,\boldsymbol{A}\,\boldsymbol{S} + \Sigma_j g_n \mu_N\, \boldsymbol{B}\boldsymbol{I} \qquad [13]$$

Analysis of a spectrum amounts to identifying which interactions are involved. The origin of the various terms in this spin Hamiltonian will be examined below. For example, changes in the g factor are shown for a variety of paramagnetic species in Table 1.

The *g* Tensor: Significance and Origin

The main reason for the deviation in g values comes from a spin–orbit coupling that results in an orbital contribution to the magnetic moment. This arises from the effect of the orbital angular momentum $\boldsymbol{L}$ which is nonzero in the case of orbitals exhibiting p, d or f character. In this case the spin is no longer exactly quantized along the direction of the external field and the g value cannot be expressed by a scalar quantity but becomes a tensor. The orbital angular momentum $\boldsymbol{L}$ is associated with a magnetic momentum given by

$$\mu_L = \mu_B \boldsymbol{L} \qquad [14]$$

For a system with a doublet ($S = \frac{1}{2}$) non-degenerate electronic ground state, the interaction with the external magnetic field can be expressed in terms of a perturbation of the general Hamiltonian by the following three terms

$$H = g_e \mu_B \boldsymbol{B}\boldsymbol{S} + \mu_B \boldsymbol{B}\boldsymbol{L} + \lambda \boldsymbol{L}\boldsymbol{S} \qquad [15]$$

Table 1 Isotropic g value variations for a series $S = \frac{1}{2}$ paramagnetic species. For organic radicals the g value deviations (from g_e) are usually small, less than 1%, but for systems that contain heavier atoms, such as transition metal ions, the variations can be much larger

Species	*g value*
e^-	2.0023
$CH_3^{\bullet}$	2.0026
Anthracene radical cation	2.0028
Anthracene radical anion	2.0029
1,4-Benzoquinone radical anion	2.0047
SO_2^-	2.0056
$HO_2^{\bullet}$	2.014
$\{(CH_3)_3C\}_2NO$	2.0063
Copper(acetonyl acetate)	2.13
VO(acetonyl acetate)	1.968
Cyclopentadienyl $TiCl_2AlCl_2$	1.975

The first and second terms correspond, respectively, to the electron Zeeman and orbital Zeeman energies. The third one represents the energy of the spin–orbit coupling where λ is the spin–orbit coupling constant which mixes the ground state wavefunctions with the excited states. The extent of the interaction between $\boldsymbol{L}$ and $\boldsymbol{S}$ mainly depends on the nature of the system considered and in many instances this interaction is stronger than that between the magnetic field and the orbital angular momentum. Depending on the strength of the molecular electric field, two limiting cases can be distinguished:

a. Strong fields: $\boldsymbol{L}$ must align itself along the field so that only $\boldsymbol{S}$ can orient itself with respect to the external magnetic field and contribute to the paramagnetism. In this case $g = g_e$. Many organic radicals or systems in which the unpaired electron is in a molecular orbital delocalized over a large molecule experience this situation.
b. Weak fields: $\boldsymbol{L}$ is no longer under the constraint of this weak field and the spin–orbit coupling $\boldsymbol{L} + \boldsymbol{S}$ can take place, giving a resultant total angular momentum:

$$\boldsymbol{J} = \boldsymbol{L} + \boldsymbol{S} \qquad [16]$$

associated with the magnetic moment:

$$\mu_J = -g_J \mu_B \boldsymbol{J} \qquad [17]$$

where g_J is called the Landé g factor. This situation occurs in the rare earth elements.

When intermediate fields are present in the paramagnetic centre, $\boldsymbol{L}$ is only partially blocked by the molecular field (transition metal ions, inorganic radicals). The system must be treated in terms of the perturbation Hamiltonian in eqn [6] which can be written as

$$H = \mu_B \boldsymbol{B}\boldsymbol{g}\boldsymbol{S} \qquad [18]$$

The g_e scalar value reported in eqn [6] is now replaced by $\boldsymbol{g}$, a second rank tensor which represents the anisotropy of the interaction between the unpaired electron and the external magnetic field and also outlines the fact that the orbital contribution to the electronic magnetic momentum may be different along different molecular axes.

The g tensor may be depicted as an ellipsoid whose characteristic (principal) values (g_{xx}, g_{yy}, g_{zz}) depend upon the orientation of the symmetry axes of the paramagnetic entity with respect to the applied magnetic field (Figure 4). The most general consequence of the anisotropy of g, from an experimental point of view, is therefore that the resonance field of a paramagnetic species, for a given frequency, depends on the orientation of the paramagnetic centre in the field itself. The g value for a given orientation depends on ϕ and θ values according to

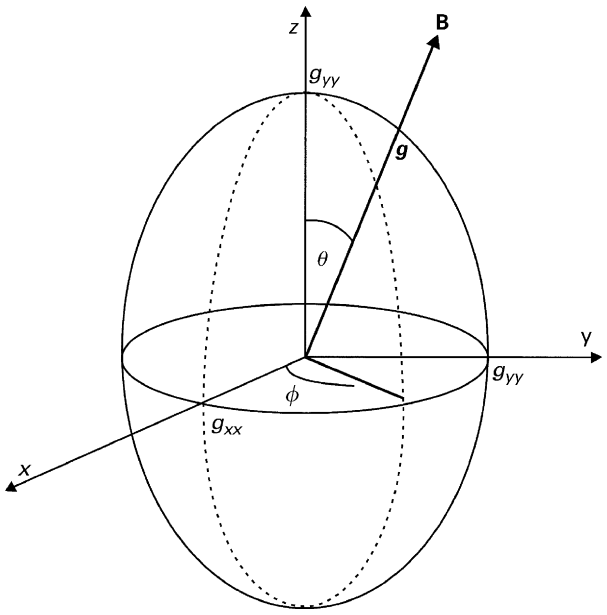

Figure 4 Orientation of the magnetic field ***B*** with respect to the ***g*** tensor ellipsoid in the crystallographic frame *x*, *y*, *z*. The characteristic angles θ and ϕ define the orientation of ***B*** which leads to the ***g*** (θ,ϕ).

the relation $g^2 = g_{xx}{}^2 \cos^2\phi \sin^2\theta + g_{yy}{}^2 \sin^2\phi\cos^2\theta + g_{zz}{}^2 \cos^2\theta$. Accordingly, the Zeeman resonance will occur at field values given by

$$B_{res} = h\nu/\mu_B(g_{xx}{}^2\cos^2\phi \sin^2\theta + g_{yy}{}^2\sin^2\phi \cos^2\theta + g_{zz}{}^2\cos^2\theta)^{-1/2} \quad [19]$$

In the most general case, the resonance observed for a paramagnetic centre in a single crystal is obtained at distinct field values of B_x, B_y and B_z when the magnetic field is parallel to the *x*, *y* or *z* crystal axis respectively. The *g* values corresponding to these three orientations (g_{xx}, g_{yy} and g_{zz}) are the principal (diagonal) elements of the *g* tensor. When the principal axes of the crystal are not known, the *g* tensors can be labelled g_1, g_2 and g_3. Absolute determination of the *g* values may in principle be carried out by independent and simultaneous measurement of *B* and ν using a gaussmeter and a frequency meter, respectively, following the equation

$$g = h\nu/\mu_B\boldsymbol{B} \quad [20]$$

The *A* Tensor: Significance and Origin

The source of this splitting is the magnetic interaction between the electron spin and neighbouring nuclear spins, which gives rise to hyperfine structure in the spectra. It arises because a nearby magnetic nucleus gives rise to a local field, $\boldsymbol{B}_{local}$, which must be compounded with the applied magnetic field ***B*** to satisfy the EPR condition $h\nu = g_e\mu_B\boldsymbol{B}$. We must now rewrite this equation as

$$h\nu = g_e\mu_B(\boldsymbol{B} + \boldsymbol{B}_{local}) \quad [21]$$

and clearly the value of ***B*** required to achieve resonance will depend on $\boldsymbol{B}_{local}$ (i.e. the magnetic moments of the nuclei). Several nuclei possess spin and corresponding magnetic moments. The nuclear spin quantum number (*I*) of a given nucleus can assume integral or half-integral values in the range 0–6. The magnetic moment μ_n associated to a nucleus is collinear with the spin vector ***I*** according to the relation

$$\mu_n = g_n\mu_N\boldsymbol{I} \quad [22]$$

which is similar to eqn [4]; g_n is the nuclear *g* factor and μ_N the nuclear magneton which is smaller than the Bohr magneton by a factor of 1838, i.e. the ratio of the mass of a proton to that of an electron.

When the paramagnetic centre contains one or more nuclei with non-zero nuclear spin ($I \neq 0$), the interaction between the unpaired electron and the nucleus with $I \neq 0$ produces further splittings of the Zeeman energies and consequently there are new transitions, which are responsible for the so-called hyperfine structure of the EPR spectrum.

Let us consider the proton as a case in point; it is a spinning positive charge and has its own associated magnetic field and consequently can interact with both the external magnetic field (cf. NMR) and that of the electron, i.e. it has a nuclear spin $I = \frac{1}{2}$ and $M_I = \pm\frac{1}{2}$. This leads to a situation whereby the energy of the system can either be lowered or be raised depending on whether the two spins are parallel or antiparallel. The energy of an electron with spin quantum number M_S and a nucleus with spin quantum number M_I is given by

$$E(M_I, M_S) = g_e\mu_B BM_S - g_N\mu_N BM_I + hA_0M_SM_I \quad [23]$$

where A_0 is the isotropic coupling constant. The first term in the equation gives the contribution due to the interaction of an electron with an applied field, giving rise to two electron Zeeman levels. The second term is the contribution due to the interaction of the nucleus with the applied magnetic field, the nuclear Zeeman levels (**Figure 5**). The final term is the energy of interaction between the unpaired electron and the magnetic nucleus. If we now substitute the values for M_S and M_I then the interaction, between an unpaired electron ($S = \frac{1}{2}$) and a single proton ($I = \frac{1}{2}$), gives rise to four energy levels, E_1 to E_4. These are calculated to be

$$E_1 = \tfrac{1}{2}g_e\mu_B B - \tfrac{1}{2}g_N\mu_B B + \tfrac{1}{4}hA_0 \quad \begin{matrix} M_S & M_I \\ +\frac{1}{2} & +\frac{1}{2} \end{matrix} \quad [24]$$

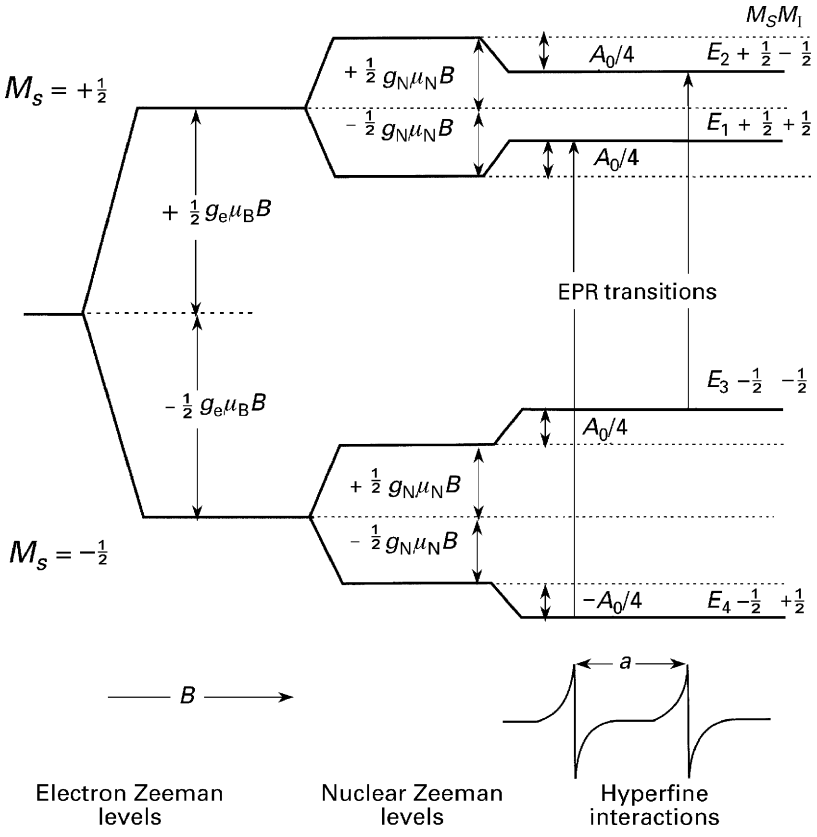

Figure 5 Energy level manifold in a high magnetic field, resulting from the interaction of an unpaired electron ($S = \frac{1}{2}$) with a nucleus of $I = \frac{1}{2}$. Note that a > 0. |a/2| < V_n.

$$E_2 = \tfrac{1}{2} g_e \mu_B B + \tfrac{1}{2} g_N \mu_N B - \tfrac{1}{4} hA_0 \quad +\tfrac{1}{2} \; -\tfrac{1}{2} \qquad [25]$$

$$E_3 = -\tfrac{1}{2} g_e \mu_B B + \tfrac{1}{2} g_N \mu_N B + \tfrac{1}{4} hA_0 \quad -\tfrac{1}{2} \; -\tfrac{1}{2} \qquad [26]$$

$$E_4 = -\tfrac{1}{2} g_e \mu_B B - \tfrac{1}{2} g_N \mu_N B - \tfrac{1}{4} hA_0 \quad -\tfrac{1}{2} \; +\tfrac{1}{2} \qquad [27]$$

The selection rules for the allowed transitions between the energy levels are

$$\Delta M_I = 0 \quad \text{and} \quad \Delta M_S = \pm 1 \qquad [28]$$

Thus two resonance transitions can occur at

$$\Delta E_A = E_1 - E_4 = g_e \mu_B B + \tfrac{1}{2} hA_0 \qquad [29]$$

$$\Delta E_B = E_2 - E_3 = g_e \mu_B B + \tfrac{1}{2} hA_0 \qquad [30]$$

These two possible transitions give rise to two absorption peaks which, at constant applied microwave frequency, occur at magnetic fields of values

$$B_1 = \frac{h\nu}{g_e \mu_B} - \frac{hA_0}{2 g_e \mu_B} = \frac{h\nu}{g_e \mu_B} - \frac{a}{2} \qquad [31]$$

$$B_2 = \frac{h\nu}{g_e \mu_B} + \frac{hA_0}{2 g_e \mu_B} = \frac{h\nu}{g_e \mu_B} + \frac{a}{2} \qquad [32]$$

where $a = hA_0/g_e \mu B$ and is the hyperfine coupling constant (HFCC) given in mT. The spectrum obtained for such a system would be a doublet centred at the g value and separated by the hyperfine coupling constant (hfc) a. If we extend the number of equivalent nuclei then the complexity of the spectrum increases in a manner described in **Table 2**. A further example is given in **Figure 6** for the radical anion of naphthalene.

It is now necessary to examine the mechanisms by which the hyperfine interactions arise. Two types of electron-spin–nuclear-spin interactions must be considered, of isotropic and anisotropic nature.

The Isotropic Interaction

This concerns exclusively s-type orbitals or orbitals with partial s character (such as hybrid orbitals constructed from s-type orbitals) because only these orbitals have a finite probability density at the nucleus. This mechanism is a quantum interaction related to the finite probability of the unpaired electron at the nucleus and is termed the Fermi contact interaction. The corresponding isotropic coupling constant a_{iso} is given by

$$a_{iso} = (8\pi/3 g_e g_n \mu_B \mu_N) |\psi(0)|^2 \qquad [33]$$

Table 2 Line intensities for a series of nuclei with different values of I. For the case of $I = \frac{1}{2}$ the line intensities can be described by the expansion of $(x+1)^2$ and hence follow Pascal's triangle

Nuclei	*Intensity of lines*								
$I = \frac{1}{2}$, e.g. ^{1}H									
Number of equivalent nuclei									
1	1	1							
2	1	2	1						
3	1	3	3	1					
4	1	4	6	4	1				
$I = 1$, e.g. ^{14}N									
Number of equivalent nuclei									
1	1	1	1						
2	1	2	3	2	1				
3	1	3	6	7	3	1			
4	1	4	10	16	19	16	10	4	1
$I = \frac{3}{2}$, e.g. $^{63,65}Cu$									
Number of equivalent nuclei									
1	1	1	1	1					
2	1	2	3	4	3	2	1		

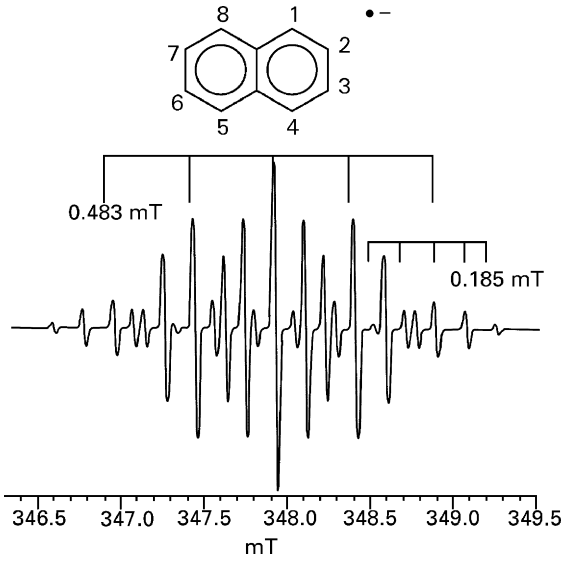

Figure 6 EPR spectrum of the radical anion of naphthalene in tetrahydrofuran as solvent. The radical was formed by dissolving naphthalene in sodium-dried tetrahydrofuran under vacuum and passing the resultant solution over a sodium metal film, again under vacuum conditions. The number of lines is given by $2nI+1$ where I equals the nuclear spin and n the number of nuclei. HFCC for 1,4,5,8 = 0.483 mT and for 2,3,6,7 = 0.185 mT.

where g_n and μ_N are the nuclear analogues of g_e and μ_B, respectively, and $|\psi(0)|^2$ is the square of the absolute value of the wavefunction of the unpaired electron evaluated at the nucleus.

Since s orbitals have a high electron density at the nucleus, the hyperfine coupling constant will be large and since s orbitals are also symmetrical it will be independent of direction. The spherical symmetry of s orbitals accounts for the isotropic nature of the contact interaction.

Thus in the case of the hydrogen atom ($M_I = \frac{1}{2}$) with 100% spin density in the 1s orbital, the EPR spectrum is composed of two resonance lines separated by approximately 50.8 mT. In the case of naphthalene, the smaller spin density associated with the ^{1}H s orbital results in a smaller isotropic coupling.

The Anisotropic Interaction

In non-spherically symmetric orbitals (p, d or f) there is no electron density at the nucleus and the electron is to be found some distance away. The interaction between it and the nucleus will be as two magnetic dipoles and consequently the interaction will be small and dependent on the direction of the orbital with respect to the applied magnetic field as well as to their separation. The coupling then arises from the classical dipolar interaction between magnetic momenta whose energy is given by

$$E = \mu_s\mu_n/r^3 - 3(\mu_s \boldsymbol{r})(\mu_n \boldsymbol{r})/r^5 \qquad [34]$$

where $\boldsymbol{r}$ is the vector relating the electron and nuclear moments and r is the distance between the two spins. The above equation gives the energy of interaction of two bar magnets if their size is small compared with the distance between them. Moving to quantum mechanics we construct the Hamiltonian by replacing the magnetic moments by the appropriate operators. The quantum mechanics analogue of eqn [34] is then obtained by replacing μ_s and μ_n by their expressions given in eqns [4] and [22]:

$$H_{aniso} = -g_e\mu_B g_n\mu_B(\boldsymbol{I}\cdot\boldsymbol{S}/r^3 - 3(\boldsymbol{I}\cdot\boldsymbol{r})(\boldsymbol{S}\cdot\boldsymbol{r})/r^5) \qquad [35]$$

Equation [35] must be averaged over the entire probability of the spin distribution. H_{aniso} is averaged out to zero when the electron cloud is spherical (s orbital) and comes to a finite value in the case of axially symmetric orbitals (p orbitals, for instance). In addition, in the case of very rapid tumbling of the paramagnetic species (as occurs in a low viscosity solution) the anisotropic term of the hyperfine interaction is averaged to zero and the isotropic term is the only one observed.

Combination of Isotropy and Anisotropy

Since any orbital may be considered as a hybrid of suitable combinations of s, p or d orbitals, so also may a hyperfine coupling be divided into a contribution arising from p or d orbitals (anisotropic) and s orbitals (isotropic). In general both isotropic and anisotropic hyperfine couplings occur when one or more nuclei with $I \neq 0$ are present in the system. The whole interaction is therefore dependent on orientation and must be expressed by the second rank A tensor as given in eqn [13]. The A tensor may be split into

anisotropic and isotropic parts as follows

$$\boldsymbol{A} = \begin{vmatrix} A_1 & 0 & 0 \\ 0 & A_2 & 0 \\ 0 & 0 & A_3 \end{vmatrix} = a_{\text{iso}} + \begin{vmatrix} T_1 & 0 & 0 \\ 0 & T_2 & 0 \\ 0 & 0 & T_3 \end{vmatrix} \qquad [36]$$

with $a_{\text{iso}} = (A_1 + A_2 + A_3)/3$. In a number of cases, the second term of eqn [36] is a traceless tensor ($T_1 + T_2 + T_3 = 0$) and has the form ($-T, -T, +2T$). The anisotropic part of the A tensor corresponds to the dipolar interaction as expressed by the Hamiltonian in eqn [13]. The s and p character of the orbital hosting the unpaired electrons are given by the following relations:

$$c_S{}^2 = a_{\text{iso}}/a_0 \quad \text{and} \quad c_P{}^2 = b/b_0 \qquad [37]$$

where a_0 and b_0 are the theoretical hyperfine coupling constants (assuming pure s and p orbitals for the elements under consideration). The terms a_{iso} and b are the experimental isotropic and anisotropic coupling constants respectively.

The *D* Tensor: Significance and Origin

The spin Hamiltonian described in eqn [13] applies to the case where a single electron ($S = \frac{1}{2}$) interacts with the applied magnetic field and with surrounding nuclei. However, if two or more electrons are present in the system ($S > \frac{1}{2}$), a new term must be added to the spin Hamiltonian (eqn [13]) to account for the interaction between the electrons. At small distances, two unpaired electrons will experience a strong dipole–dipole interaction, analogous to the interaction between electron and magnetic dipoles, which gives rise to anisotropic hyperfine interactions. The electron–electron interaction is described by the spin–spin Hamiltonian given in eqn [38]:

$$H_{ss} = \boldsymbol{SDS} \qquad [38]$$

where $\boldsymbol{D}$ is a second rank tensor (the zero-field parameter) with a trace of zero. As with the $\boldsymbol{g}$ and $\boldsymbol{A}$ tensors, the $\boldsymbol{D}$ tensor can also be diagonalized so that $D_{xx} + D_{yy} + D_{zz} = 0$. Equation [38] can be added to eqn [18] to obtain the correct spin Hamiltonian for an $S > \frac{1}{2}$ system (in the absence of any interacting nucleus):

$$H = \mu_B \boldsymbol{BgS} + \boldsymbol{SDS} \qquad [39]$$

Since the trace of $\boldsymbol{D}$ is zero, calculation of the energy state for a system with $S = 1$ requires only two independent parameters which are designated $\boldsymbol{D}$ and $\boldsymbol{E}$. The spin coupling is direct in the case of organic molecules in the triplet state and biradicals, but occurs through the orbital angular momentum in the case of transition metal ions. In the latter case, the $\boldsymbol{D}$ and $\boldsymbol{E}$ terms depend on the symmetry of the crystal field acting on the ions:

$$H = D\left(S_z{}^2 - \frac{S^2}{3}\right) + E(S_x{}^2 - S_y{}^2) \qquad [40]$$

For axially symmetric molecules, the calculated shape of the $\Delta M_S = 1$ lines are given in **Figure 7a**. The separation of the outer lines is $2D'$ (where $D' = D/g\mu_B$) while that of the inner lines is D (E is zero in this case). The theoretical line shape for a randomly oriented triplet system with $E \neq 0$ is shown in **Figure 7b**. The separation of the outermost lines is again $2D'$ whereas that of the intermediate and inner pairs is $D' + 3E'/2$ and $D' - 3E'/2$ respectively. As the zero-field interactions become comparable to, and larger than, the microwave energy, the line shape exhibits severe distortions from the simulated case in **Figure 7**. Well-known examples of $S = 1$ include the excited triplet state of naphthalene with $D/hc = 0.1003\ \text{cm}^{-1}$, $E/hc = -0.0137\ \text{cm}^{-1}$ and $g = 2.0030$.

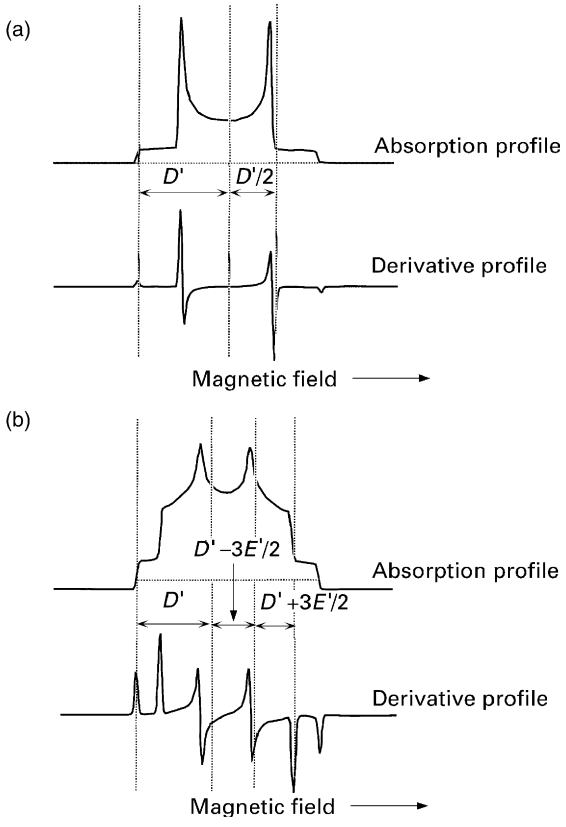

Figure 7 Theoretical absorption and first derivative spectra of the $\Delta M_S = 1$ region of a randomly oriented triplet. (a) $S = 1$ for a given value of D ($E = 0$) and isotropic g. (b) $S = 1$ where D is 6.5 times larger than E and g is isotropic.

Line Shapes and Symmetry Considerations in EPR Spectra

An important consideration in EPR is the effect of symmetry on the line shapes. In many cases the samples investigated by EPR are polycrystalline materials, composed of numerous small crystallites that are randomly oriented in space. The resultant *powder* EPR spectrum is the envelope of spectra corresponding to all possible orientations of the paramagnetic species with respect to the magnetic field; provided the resolution is adequate, the magnitude of the g and A tensor components can be extracted from the powder spectra whereas no information can be obtained on the orientation of the tensor principal axes.

The profile of the powder spectrum is determined by several parameters, including the symmetry of the g tensor, the actual values of its components, and the line shape and the line width of the resonance. Concerning the symmetry of the g tensor, three possible cases can be identified.

Isotropy of g

In this case, the g tensor is characterized by $g_{xx} = g_{yy} = g_{zz} = g_{iso}$ and a single symmetrical line is observed. This simple situation is not very often encountered in powders except for some solid state defects and transition metal ions in highly symmetric environments such as O_h or T_d.

Axial Symmetry of g

Paramagnetic species isolated in single crystals exhibit resonances at typical magnetic fields which depend on

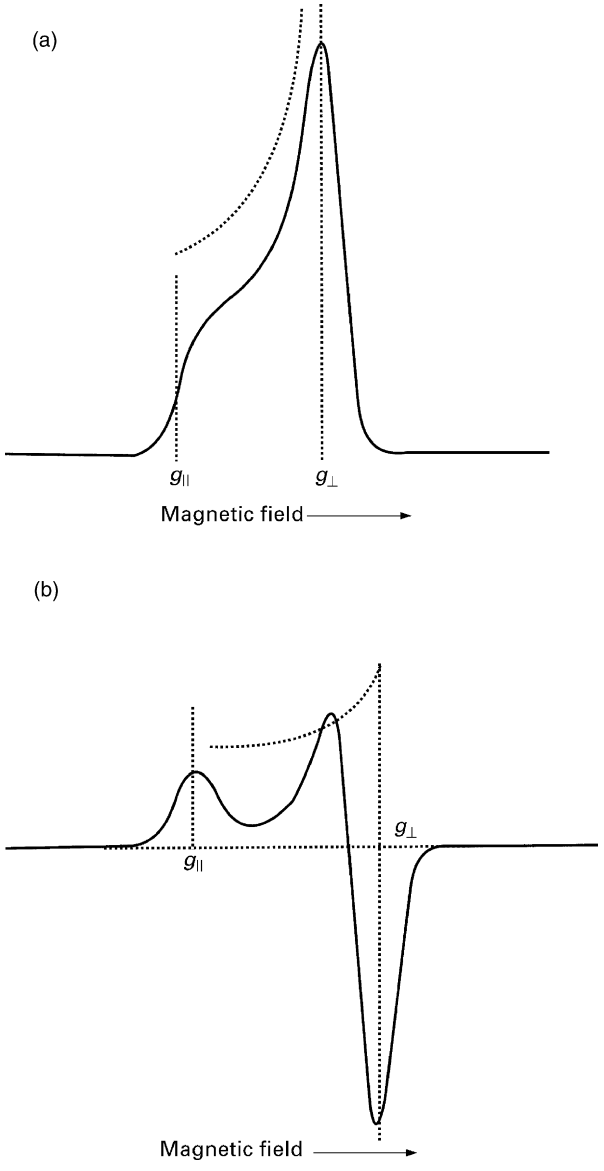

Figure 8 Powder EPR spectrum of a paramagnetic species with $I = 0$ in axial symmetry. (a) absorption profile, (b) first derivative profile. The dotted lines have been calculated by assuming a zero line width whereas the solid lines correspond to a finite line width.

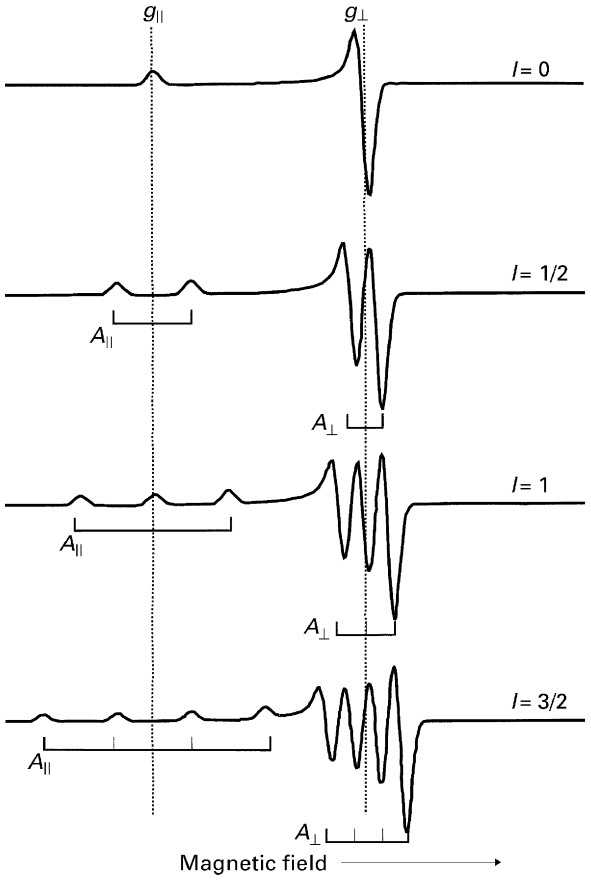

Figure 9 Effects of nuclear spin on the calculated powder EPR spectra for axial symmetry. The value of I varies from 0 to $\frac{3}{2}$. Note that the g values remain constant (illustrated by dotted lines). $\boldsymbol{g}_{\|}$ is split by $\boldsymbol{A}_{\|}$ and $\boldsymbol{g}_{\perp}$ is split by $\boldsymbol{A}_{\perp}$. The $\boldsymbol{A}_{\|}$ and $\boldsymbol{A}_{\perp}$ values remain constant.

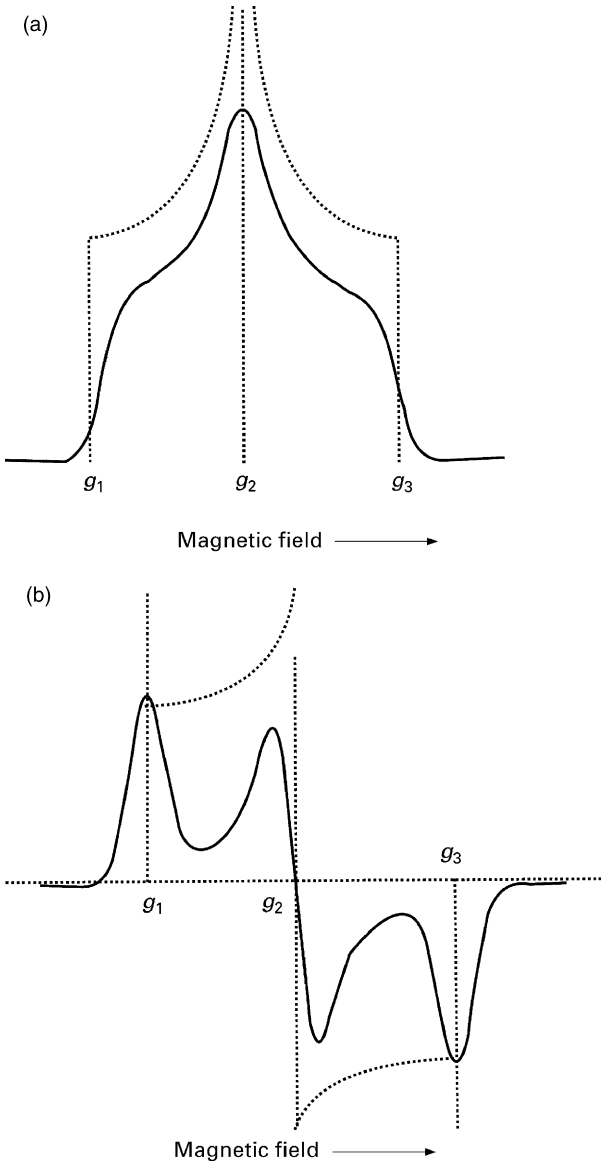

Figure 10 Powder EPR spectrum of a paramagnetic species in orthorhombic symmetry. (a) Absorption profile, (b) first derivative profile. The dotted and solid lines have the same significance as described in Figure 7.

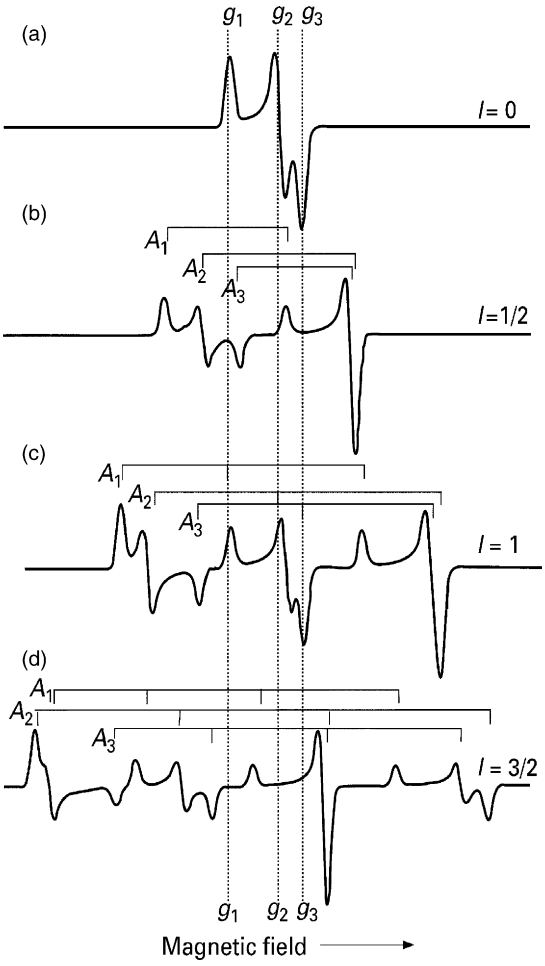

Figure 11 Effects of nuclear spin on the calculated powder EPR spectrum of a species with orthorhombic symmetry. The spectrum is anisotropic both in $\boldsymbol{g}$ and A ($\boldsymbol{g}_1$ is split by A_1, $\boldsymbol{g}_2$ is split by A_2 and $\boldsymbol{g}_3$ by A_3). The value of I varies from 0 to $\frac{3}{2}$. It should be noted that when I assumes an integer value (as in c), the features of the original $I = 0$ spectrum (a) are maintained in the centre of the spectrum. When I has half-integer values the hyperfine values are symmetrically disposed about the centre.

their orientation and are given by eqn [19]. In the particular case of axial symmetry of the system, e.g. (C_{4n}, D_{4h}), if z is the principal symmetry axis of the species and θ the angle between z and the magnetic field, the x and y directions are equivalent and the angle ϕ becomes meaningless (Figure 4). Equation [19] reduces to

$$B_{\text{res}} = h\nu/\mu_{\text{B}}(g_{\perp}^2 \sin^2\theta + g_{\parallel}^2 \cos^2\theta)^{-1/2} \qquad [41]$$

where $g_{\parallel} = g_{zz}$ and $g_{\perp} = g_{yy} = g_{xx}$ are the g values measured when the axis of the paramagnetic species is, respectively, parallel and perpendicular to the applied magnetic field.

The powder spectrum is the envelope of the individual lines corresponding to all possible orientations in the whole range of ϕ. Assuming the microcrystals are randomly distributed, simple considerations show, however, that the absorption intensity, which is proportional to the number of microcrystals at resonance for a given θ value, is at a maximum when $\theta = \pi/2$ ($B_{\perp}$) and a minimum for $\theta = 0$ ($B_{\parallel}$); this allows the extraction of the $g_{\parallel}$ and $g_{\perp}$ values, which correspond to the turning points of the spectrum. Figure 8 gives a schematic representation of the absorption curve and of its first derivative for a polycrystalline sample containing a paramagnetic centre with axial symmetry. The variation in the spectral profile for the same species as M_I varies is also shown in Figure 9.

Orthorhombic Symmetry of *g*

Three distinct principal components are expected in the case of a system with orthorhombic symmetry, e.g. (D_{2h}, C_{2v}). For polycrystalline samples, the absorption curve and its first derivative exhibit three singular points, corresponding to g_1, g_2 and g_3 (**Figure 10**). For powder spectra the assignments of g_1, g_2 and g_3 to the components g_{xx}, g_{yy} and g_{zz} related to the molecular axes of the paramagnetic centre is not straightforward and must be based on theoretical grounds or deduced from measurements of the same paramagnetic species in a single crystal. The situation becomes much more complicated in the presence of nuclei with $I \neq 0$. In several cases an initial interpretation of the experimental data can be achieved by using a simple analysis for the $\boldsymbol{g}$ tensor and neglecting second-order effects since the $\boldsymbol{A}$ tensor has the same type of angular dependence as the $\boldsymbol{g}$ tensor. Provided the principal axes are the same, then each of the three possible lines of the $\boldsymbol{g}$ tensor (g_1, g_2 and g_3) will be split into a number of lines that depend on the nuclear spin with the spacing corresponding to the appropriate component of the $\boldsymbol{A}$ tensor (A_1, A_2 or A_3); g_1 is split by A_1, g_2 is split by A_2 and g_3 is split by A_3 (**Figure 11**).

Summary

The basic principles of EPR spectroscopy have been outlined. Although far from being an exhaustive treatment of the subject, it provides the reader with essential knowledge of the technique and is a useful stepping stone for the articles on methods and instrumentation and applications.

See also: Chemical Applications of EPR, EPR Imaging, EPR, Methods, NMR in Anisotropic Systems, Theory, NMR Principles, NMR Relaxation Rates.

Further Reading

Abragam A and Bleaney B (1970) *Electron Paramagnetic Resonance of Transition Ions*. Oxford: Oxford University Press.

Atherton NM (1993) *Principles of Electron Spin Resonance,* PTR Prentice Hall Physical Chemistry Series. Englewood Cliff, NJ: Prentice-Hall.

Bolton JR, Weil JA, and Wertz JE (1994) *Electron Paramagnetic Resonance: Elementary Theory and Practical Applications*. New York: Wiley-Interscience.

Che M and Giamello E (1987) In: Fieno JLG (ed.) *Spectroscopic Characterization of Heterogeneous Catalysts. Part B: Electron Paramagnetic Resonance*, vol. 57. Amsterdam: Elsevier Science Publishers.

Mabbs FE and Collison D (1992) *Electron Paramagnetic Resonance of d-Transition Metal Compounds*. Vol 16 in Studies in Inorganic Chemistry. Amsterdam: Elsevier.

Pilbrow JR (1993) *Transition Ion Electron Paramagnetic Resonance*. Oxford: Clarendon Press.

Symons MRC (1978) Chemical and biological aspects of electron spin resonance spectroscopy. *Chemical Aspects of Physical Techniques*. New York: Van Nostrand Reinhold.